

# Optical Array Fabrication via Photoimaging of Acrylate Monomers

*Paul M. Ferm, Kevin Battell, Karl Beeson, Robert Blomquist, Arthur Martin, Macrae Maxfield, Michael McFarland, and Scott Zimmerman  
AlliedSignal MicroOptic Devices, Morristown, New Jersey*

## Abstract

A process technology has been developed in which dense arrays of high aspect ratio, high resolution optical elements can be fabricated directly using acrylate monomers. The technique offers flexibility in optical element design. Pilot plant scale development was pursued to commercialize products for the LCD industry based on this technology. Ultimately, business and technical limitations resulted in new fabrication strategies being put in place, but the photolithographic technique was seen to be capable of impressive imaged micro-optic structures.

## Introduction

Photoresist technology is highly developed for the semiconductor and display industries in which thin, high resolution structures are produced, commonly as a sacrificial masking step to allow etching or application of other materials. Intricate 3-dimensional photoresist microstructures have been created by photomask imaging for possible mechanical and optical applications.<sup>1</sup> Stereolithography has emerged as a powerful 3-D prototyping tool of macrostructures and is based on photopolymerization of monomers via laser rastering.<sup>2</sup> There is a growing need to supply mass produced micro-optical elements to several market segments, including display lighting and diffusing elements, specialty lighting, holography, and optical waveguides for hybrid integrated circuits. Linear and crossed arrays of optical elements made via compression molding or photopolymer casting from a master tool are already in the marketplace as projection TV viewing screens and LCD brightness enhancement films. The direct photolithographic production of micro-optical elements have been pursued in the holographic industry and techniques have been developed in which both bulk and surface photopolymerization are utilized and followed by mass transport development.<sup>3</sup> The creation of optical waveguide circuits using photopolymers is underdevelopment at AlliedSignal, Inc. and was the seminal work for the technology discussed below.<sup>4</sup>

The subject of this paper is the direct photolithographic production of arrays of optically clear elements designed to significantly improve LCD system performance. In this approach, light is extracted into a narrow angular cone from

a planar waveguide sheet using a collimation film and is transmitted through the LCD cell, which is well optimized for collimated light. The light exiting the LCD is then evenly distributed to wide angles by a diffusing film and thus produces only properly rendered colors at all viewing angles.<sup>5</sup> To maintain the highest possible LCD system efficiency, a bulk diffuser material is not acceptable since it scatters light in both the forward and reverse directions and creates substantial diffuse reflectance of ambient light. Instead, a tapered optical waveguide with height to width ratios greater than 3:1 was chosen. The tapered wall results in an output light emitting surface of about half the width of the input surface and transmitted light is forced to undergo a series of reflections which creates the desired, final angular light distribution. The target optical structure which is the main topic of this paper is defined in detail elsewhere.<sup>6</sup> Key to the optical efficiency of the resulting system is the maximization of the fill factor of the base, which defines the optical aperture of the array. Ideally, the sidewalls come to a knife edge between adjacent elements. After creating the optical array, a low index black material is applied between the structures. The blackfill serves many purposes: it acts as a low index total internal reflection boundary layer to guide the desired light through the optical elements, it absorbs any undesirable, high angle light from the backlight, it presents a black front surface to reduce diffuse reflection of ambient light, and it adds structural rigidity to the optical array.

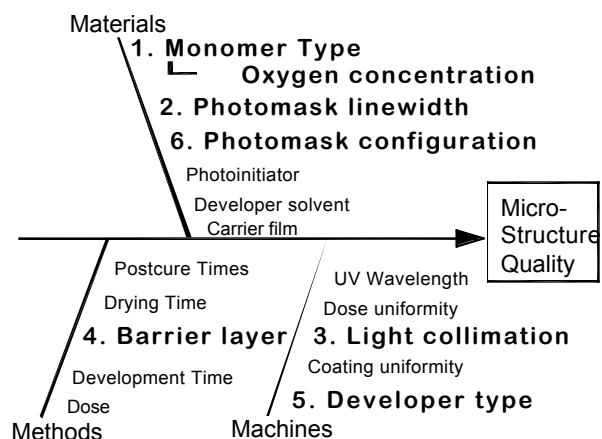


Figure 1. Cause and effect diagram listing key variables for photolithographic micro-optic array process.

## The Photopolymerization Process

When UV light interacts with photocuring resin, a large number of variables can affect the shape and quality of the resulting structures. A cause and effect diagram of some of the variables determined to be critical is shown in Figure 1. The numbered variables in this figure will each be discussed below.

### 1. Effect of monomer and oxygen

The monomer used in this work consisted of two acrylates, EBDA oligomer (ethoxylated bisphenol A diacrylate) and TMPTA monomer (trimethyl propane triacrylate), in a 2:1 blend by weight. Irgacure 651 photoinitiator was used in 1% to 6% loadings by weight. To create arrays of tapered optical elements, a photomask with a square grid of lines was employed. Typically, a pitch of 50  $\mu\text{m}$  was chosen and linewidths were varied from 5 to 15  $\mu\text{m}$ . For production of a flexible array, a carrier web was attached to the photomask and then coated with monomer. Polymerization can take place under atmospheric oxygen conditions or isolated from atmosphere with a barrier layer, depending on the type of structure being created. UV radiation was provided by a 30°-diagonal, collimated, mercury light source, with an intensity of 10 to 30  $\text{mW}/\text{cm}^2$  as measured with a  $360 \pm 25$  FWHM nm radiometer probe. The structure is then developed with methanol, dried, and post-cured.<sup>7</sup>

The choice of acrylate monomer, especially its shrinkage upon cure and its oxygen content, is a key enabling element in the creation of tapered or shaped structures. The acrylate blend used here exhibits densities increases from 1.134 to 1.218  $\text{g}/\text{ml}$  upon polymerization. This densification is accompanied by an index of refraction increase from 1.521 to 1.546. Due to these material changes, the light beam undergoes self-focusing during the polymerization process. Studies of such systems with a Gaussian beam waist laser have been reported.<sup>8</sup> The polymerization is intensity dependent and in the work presented here, the UV radiation intensity was always such that self focusing was active. The self-focusing effect could be reduced or eliminated by using higher intensity laser beams and imaging directly with the laser beam profile or through a mask. Practical illumination was always carried out with a mercury lamp and a photomask.

The effect of oxygen on quenching the free radical photopolymerization process is well documented for both single elements made with a Gaussian laser beams<sup>8</sup> and in the curing of coating films.<sup>9</sup> The effect of oxygen in the creation of dense optical arrays leads to unique phenomena. The evolution of the growth of the tapered structures was captured in a series of SEM photographs shown in Figure 2. Here the monomer blend was applied to a photomask and then a top glass plate was pressed onto 125  $\mu\text{m}$  shims. The exposure dose was terminated after 0.36, 0.46, and 0.56 millisecond exposures at 30  $\text{mW}/\text{cm}^2$  for three separate

samples which were developed and postcured. Even though at time zero, the light was evenly distributed through the square aperture, the polymerization initiated in the center of each square. It is believed that the oxygen is dynamically depleted uniformly throughout the open aperture, but the facile diffusion of oxygen from the dark region sets up an oxygen concentration gradient. Polymerization first occurs then at the center of the open aperture where oxygen content is lowest. Polymerization then proceeds both vertically and laterally (as seen by comparing the Figures 2(a) and 2(b)) as the oxygen is depleted in these regions, until the structure terminates into the barrier layer, which in this case was a glass plate. The photopolymerization is sharply non-linear as witnessed by the growth in the last 0.1 seconds versus the initial 0.46 seconds. If grossly overexposed, the structures grow together in the dark regions.

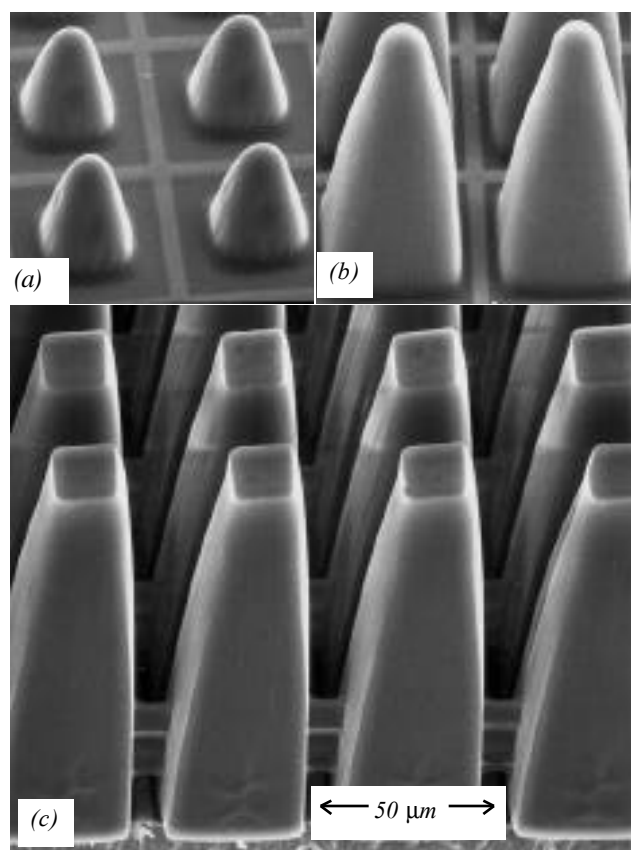


Figure 2. SEM images illustrating the evolution of microstructure formation at three exposure doses. (a) 0.26 sec, (b) 0.36 sec and (c) 0.46 sec. Elements have 50  $\mu\text{m}$  pitch.

### 2. Effect of Photomask linewidth

For use as an LCD light diffuser, the ideal optical array must provide the smallest possible interstitial region between adjacent tapered waveguides (and thus the highest fill factor). The photomask line width is a key variable which determines fill factor. Figure 3 shows the effects of

using 5 and 15  $\mu\text{m}$  lines on 50  $\mu\text{m}$  centers. The exposure conditions are optimized in each case to ensure that the polymerization is driven to the barrier layer and precisely terminated to get the best combination of smooth, firm tips and minimal residual material between structures. Figure 3 shows the dramatic effect of linewidth choice on fill factor, wall angle, and residual material. The effect of linewidth on wall angle indicates that the interaction between the dynamic local oxygen concentration and mask linewidth is significant. These structures were grown on a carrier film. The polyester (0.001 to 0.004 inch PET) carrier film was temporarily bonded to the photomask using a solvent, such as water or alcohol, to index match the interfaces and provide intimate contact. Due to the non-linear nature of the photopolymerization, vacuum contacting could not be used since the resulting Newton rings resulted in varying structure dimensions which could not be observed with microscopy, but were immediately apparent as macroscopic cosmetic defects.

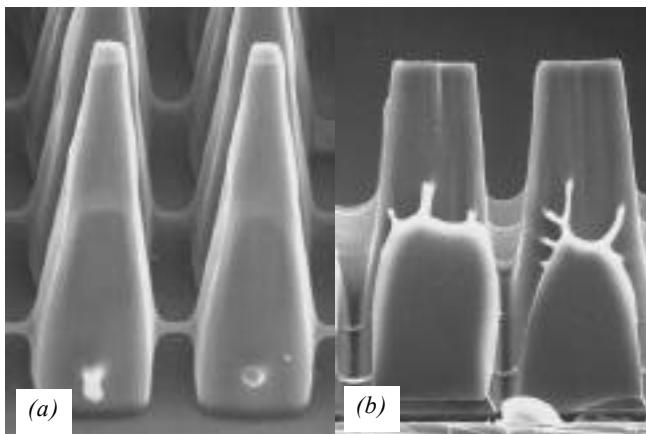


Figure 3. Images showing effect of photomask linewidth on amount of residual photopolymer between adjacent array elements. (a) 15  $\mu\text{m}$  linewidth, (b) 5  $\mu\text{m}$  linewidth. (50  $\mu\text{m}$  pitch)

### 3. Effect of light collimation

When a  $\pm 2$  degree collimated light beam was used together with a carrier web, microscopic internal structures called striations were created which resembled fibers or waveguides within the photopolymer structures. These internal striations would then be developed and result in vertical ridges along the edge of the waveguides. These striations were found to be an interaction effect of the UV radiation collimation and the haze of the carrier web. It is hypothesized, that the collimated light is effectively focused by the birefringent inhomogeneities in the PET film to create local hot spots. The hot spots then create internal regions of higher cross-link density which have different solubility during development. Several techniques were examined to eliminate this phenomenon. Most successful, was the inclusion of a  $2^\circ$  to  $10^\circ$  FWHM diffuser in the optical path. The effect was to smooth out the local hot

spots created by the carrier web inhomogeneities. Figure 4 shows a rectangular microstructure with pronounced sidewall striations.

### 4. Effect of barrier layer

An oxygen barrier layer was provided by a top PET web which was applied to the monomer coating after it was applied with a traversing precision slot die. This barrier layer enabled the creation of a smooth tip. In the case when the surface quality is not critical or a rough surface is desired, exposure of the structure under air was possible and simplified the coating process. The roughness of the tip is induced by atmospheric oxygen. The monomer epilayer is never sufficiently crosslinked and the UV hot spots and internal striations interact to create an unevenly polymerized tip. Figure 5 shows the such a microstructure tip after development.

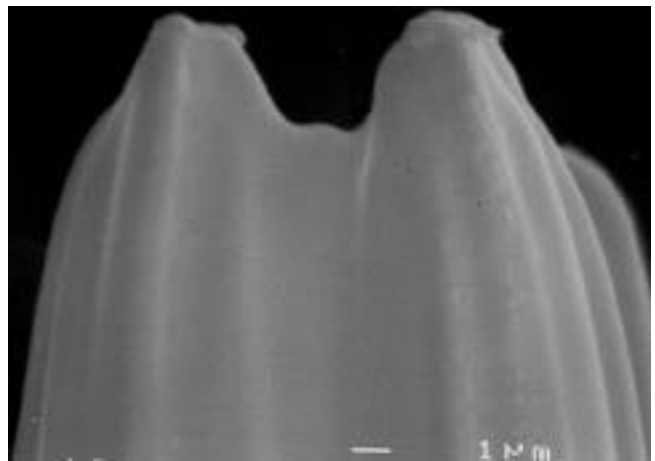


Figure 4. SEM image showing uneven tip of a photopolymer structure that was created while exposed to air.

### 5. Effect of development method

Another important process variable related to the optical surface quality of the resulting structure was the development method employed. Development was one of the most difficult lab to pilot transitions due to the scaling up of solvent volume, flow rates, and turbulence. Turbulence was found to lead to cosmetic nonuniformities. The best solution was found in the implementation of laminar flow of solvent across the structures. The pilot facility was built to handle a 24" diagonal active area and the developer tanks were cascaded, with the final tank having the highest purity solvent. Air knives were used to remove the bulk of the liquid before the film entered dryers and nitrogen-purged postcure units. More aggressive developer technologies, such as nozzles and flobars were also investigated, but were found to be too aggressive for the partially cured structures and the turbulence typical of these systems resulted in cosmetically unacceptable features.

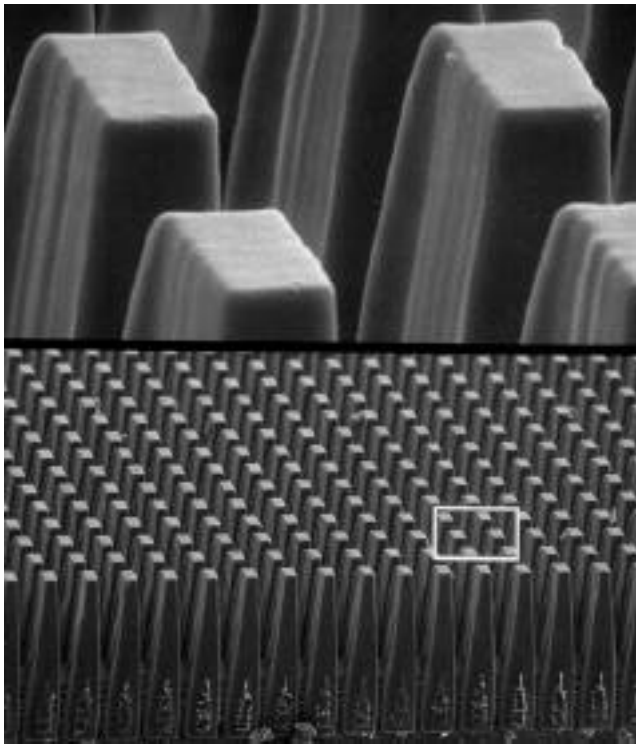


Figure 5. SEM image of rectangular optical array elements highlighting sidewall striations. (50  $\mu\text{m}$  pitch)

## 6. Photomask configuration

The configuration of the mask, in ways other than the simple variation of linewidth, was a very significant variable affecting product shape and performance. For instance, in order to smooth the far-field angular light distribution, small structures were included within the open aperture of the photomask. Figure 6 compares the shape of the tips of microstructures that were created with a normal, open square aperture to that of the identical mask with an opaque cross (5 x 20  $\mu\text{m}$  lines) in the center of the aperture. The resulting photopolymer structure is not only distinguished by a cross-shaped tip, but also contained internal index gradients which further affected light propagation.

### Pilot facility microstructures

In the developed pilot process, a carrier film was contacted temporarily to a photomask, and acrylate photopolymer was coated, exposed, and then transported to development and postcure. The pilot facility was set up as a batch process on a continuous web to allow consecutive contacts with a photomask followed by immediate transfer of the optical array into development. Throughputs of 1000 - 15" diagonal panels/day were attained, with each panel containing over 25 million individual optic elements. Array cosmetics was a challenging area to put under control, but ultimately, attention to all details of monomer coating uniformity, developer flow uniformity, and drier uniformity provided for

cosmetically perfect arrays. Profiles offer the best overall view of the structures, but the top view of the alignment of the structure tips was also an important response variable. During the development of the process, the tips of the cones were often off of their nominal centers. Random alignment of tips resulted in cosmetic defects in optical arrays. The amount of misalignment was significantly affected by the residual photopolymer between structures. Heavy residual material resulted in more misalignment and cosmetic defects. When smaller linewidths are used, the exposure dose must be overcompensated to eliminate tip misalignment. The resulting fill factor is the same as for a larger linewidth mask (with the structure being "weaker" and less robust to development). The specified optical array called for fill factors of 80% or more for the desired LCD viewing screen application. The pilot scale process technology ultimately provided too small of a base fill factor to achieve sufficient optical transmission for this application.

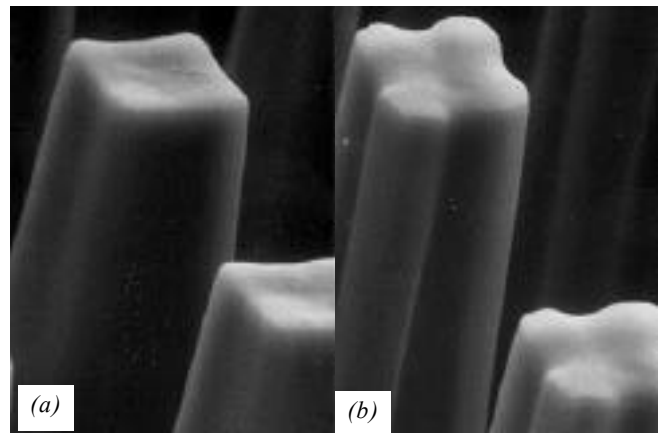


Figure 6. SEM Images showing shape of microstructure tip created with two different square grid photomasks, (a) clear aperture, (b) aperture containing cross. (50  $\mu\text{m}$  pitch)

### Process flexibility to create novel shapes

As a final note on the flexibility of this processing technology, Figure 7 shows an array of lenses that were created using the same basic materials and exposure conditions. Here the mask pitch was increased to 750  $\mu\text{m}$ . The monomer was coated to 500  $\mu\text{m}$  and no barrier film was used. A 20° to 40° FWHM light diffuser was used to create a broadly divergent light distribution and exposures of 150 - 300  $\text{mJ}/\text{cm}^2$  were applied. Under these conditions, the variables of mask pitch and light diffusion were balanced with a continual supply of oxygen to the dark regions between open apertures to create a rounded lens structure. The curvature of this lens could be controlled by adjusting these variables. Other shapes could also be created and were limited only by the creativity of the experimenter in adjusting the UV light distribution, light declination angle, photomask configuration, photoinitiator level, and oxygen gradients within the film.

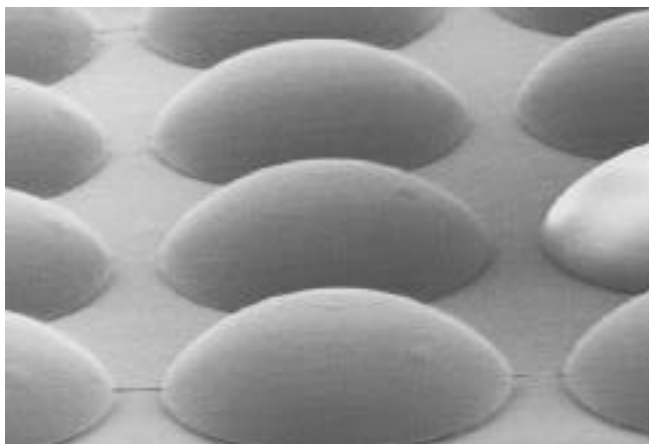


Figure 7. SEM Image of photopolymer lens array. (750  $\mu\text{m}$  pitch)

### Conclusion

For the creation of the targeted micro-optical array for LCD applications, the technical limitations described above coupled with business considerations have resulted in the selection of new fabrication strategies. However, the process developed here has the ability to create a wide range of optical structures. Optical surface quality can be excellent and shapes are attainable which cannot be made by even the most precise machining techniques. In particular, the creation of closely spaced structures with wall angles  $4^{\circ}$ - $8^{\circ}$

from normal and aspect ratios of 3:1 to 5:1 are possible. Of the many significant process variables, the ones highlighted here include oxygen concentration, photomask linewidth and configuration, carrier film, barrier layer, light collimation, and developer configuration. These key process variables offer a versatile toolbox for the creation of novel micro-optical arrays using photopolymerization.

### References

1. W. Feely, *SPIE Vol. 631* (1986) 48.
2. J. C. André, A. LeMehaute, and O. De Witte, *French Patent 8411241*, 1984.
3. See "Radiation Curing", S. Peter Pappas, 1992, Plenum Press, New York for a broad description of the science and technology of this field.
4. L. Eldada, C. Xu, K. Stengel, L. Shacklette, and J. Yardley, *J. Lightwave Tech.*, **14** (1996) 1. Also see L. Eldada, K. Stengel, L. Shacklette, R. Norwood, C. Xu, C. Wu, and J. Yardley, *SPIE 3006* (1997) 344.
5. S. Zimmerman, K. Beeson, M. McFarland, J. Wilson, T. J. Credelle, K. Bingaman, P. Ferm, J. Yardley, *Journal of SID*, **3/4** (1995) 173.
6. S. M. Zimmerman, K. W. Beeson, M. McFarland, J. T. Yardley, and P. M. Ferm, *U.S. Patent 5,481,385* (1996).
7. K. Beeson, S. Zimmerman, P. Ferm, M. McFarland, *U.S. Patent 5,462,700* (1995).
8. A. Kewitsch and A. Yariv, *Optics Letters*, **21**, (1996) 24 and Y. Brulle, A. Bouchy, B. Valance, and J. Andre, *J. Photochem. Photobiol. A: Chem.*, **83** (1994) 29.
9. M. A. Paczkowski, I. Nunez, L. Falanga, and J. Sharma, *Radtech '94 North America Proceedings*, **2** (1992) 647.